

Comparing Methods of Barometric Efficiency Characterization for Specific Storage Estimation

by Chris Turnadge¹, Russell S. Crosbie², Olga Barron³, and Gabriel C. Rau^{4,5}

Abstract

Groundwater responses to barometric pressure fluctuations are characterized using the concept of barometric efficiency (BE). For semiconfined and confined aquifers, BE values can be used to provide efficient, low-cost estimates of specific storage. This study compares, for the first time, eight existing methods of BE estimation. Comparisons were undertaken using data from the Peel region of Western Australia. Fourier analysis and regression deconvolution methods were used to estimate aquifer confinement status. The former approach was found to be robust and provided a quantitative basis for spatial comparisons of the degree of confinement. The latter approach was confounded by the presence of diurnal and/or semidiurnal signals. For wells at which semiconfined or confined responses were identified, frequency and time domain methods were used to estimate BE values. Most BE estimation methods were similarly confounded by diurnal and/or semidiurnal signals, with the exception of the Acworth et al. (2016) method. Specific storage values calculated from BE values were order-of-magnitude consistent with the results of four historical pumping tests. The methods implemented in this research provide efficient, low-cost alternatives to hydraulic testing for estimating aquifer confinement, as well as the BE and specific storage of semiconfined and confined aquifers. The frequency and duration of observations required by these methods are minimal; for example, typically requiring a minimum of four observations per day over a four month period. In some locations they may allow additional insights to be derived from existing groundwater hydrograph data.

Introduction

The response of groundwater pressures to barometric pressure fluctuations (Jacob 1940), Earth and ocean tides (Ferris 1952; Bredehoeft 1967), seismic waves (Cooper et al. 1965), and mechanical loading at the ground surface (van der Kamp and Schmidt 2017) have been recognized for over 100 years (e.g., Veatch 1906). McMillan et al. (2019) provided a comprehensive overview of this topic. Groundwater responses to barometric pressure fluctuations can be characterized using the metric of barometric efficiency (BE), which is calculated using the ratio of (1) instantaneous changes in groundwater pressure to (2) changes in barometric pressure at the ground surface. A

range of BE estimation methods have been developed and applied to various hydrostratigraphic unit types, including confined and unconfined aquifers, fractured rock aquifers, and aquitards (Table 1). Linear regression is by far the most commonly used method. Other popular approaches are the Clark (1967) and related Rahi (2010) methods, both of which use sets of defined rules when iteratively calculating BE values. Various frequency domain (Quilty and Roeloffs 1991; Acworth and Brain 2008; Acworth et al. 2016) and regression deconvolution methods (Rasmussen and Crawford 1997) have also been developed. Less commonly used are graphical methods (Rhoads and Robinson 1979; Gonthier 2007) which are based on bivariate plots of groundwater and barometric pressures, known as scribble plots (Kilroy 1992). Consistent elliptical patterns are commonly observed in such plots; slopes of the principal axes of these ellipses provide estimates of BE. Analytical modeling (Odling et al. 2015) and numerical modeling (Seo 1999) have also been used to interpret groundwater pressure responses.

Other than a handful of exceptions (Rhoads and Robinson 1979; Rasmussen and Crawford 1997; Augustine 2015; Odling et al. 2015), comparisons of BE estimation have only considered two or three methods. Assessments of aquifer confinement status (in order to ensure semi-confined or confined conditions) when using time series methods have also been limited (e.g., Rahi and Halihan 2013; Acworth et al. 2015; Dong et al. 2015).

¹Corresponding author: CSIRO Land and Water, Locked Bag 2, Glen Osmond, SA 5064, Australia; chris.turnadge@csiro.au

²CSIRO Land and Water, Locked Bag 2, Glen Osmond, SA, 5064, Australia.

³CSIRO Land and Water, Private Bag 5, Wembley, WA, 6913, Australia.

⁴Institute of Applied Geosciences, Karlsruhe Institute of Technology, Kaiserstrasse 12, 76131, Karlsruhe, Germany.

⁵Connected Waters Initiative Research Centre, University of New South Wales, Kensington, NSW, 2052, Australia.

Article impact statement: Existing methods of quantifying barometric efficiency were compared and used to estimate aquifer specific storage.

Table 1
Summary of Published Analyses of Groundwater Pressure Responses
to Atmospheric Barometric Fluctuations

Context	Publication	Study Location	Method(s) Used
Confined aquifer	Robinson and Bell (1971)	Appalachian Mountains, USA	LR
	Rhoads and Robinson (1979)	Virginia, USA	GR, LR, DMA
	Galloway and Rojstaczer (1988)	Yucca Mountain, Nevada, USA	Q&R
	Robson and Banta (1990)	Colorado, USA	CLK
	Beavan et al. (1991)	Aswan, Egypt	Unclear
	Geldon et al. (1997)	Yucca Mountain, Nevada, USA	LR
	Rasmussen and Crawford (1997)	Savannah River Site, USA	LR, D&R, R&C
	Seo (1999)	Iowa, USA	LR, NM
	Hobbs and Fourie (2000)	Vaal River Barrage, South Africa	LR
	Sahu (2004)	Ohio, USA	LR
	Rasmussen and Mote (2007)	Savannah River Site, USA	LR, R&C
	Rahi and Halihan (2009)	Oklahoma, USA	RAH
	Butler et al. (2011)	Kansas, USA	R&C
	Darner and Sheets (2012)	Great Lakes Region, USA	CLK
	Hussein et al. (2013)	East Yorkshire, UK	Q&R
	Odling et al. (2015)	East Yorkshire, UK	Q&R, AM, NM
	Augustine (2015)	Alberta, Canada	LR, CLK, RAH, GR, R&C
	Dong et al. (2015)	Kyushu, Japan	CLK
	Fuentes-Arreazola et al. (2018)	Baja California Peninsula, Mexico	RAH
	Acworth and Brain (2008)	New South Wales, Australia	A&B, GR
	Acworth et al. (2015)	New South Wales, Australia	A&B
	Acworth et al. (2016)	New South Wales, Australia	ACW
Acworth et al. (2017)	New South Wales, Australia	ACW	
Turnadge et al. (this article)	Western Australia, Australia	AoR, MoR, LR, CLK, RAH, Q&R, ACW, R&C	
Unconfined aquifer	Hare and Morse (1997)	New York State, USA	LR
	Hare and Morse (1999)	New York State, USA	LR
	Barr et al. (2000)	Saskatchewan, Canada	BAR
	Lee and Lee (2000)	Wonju, South Korea	Q&R, CLK
	Spane and Mackley (2011)	Washington State, USA	R&C
	Rau et al. (2018)	New South Wales, Australia	ACW
Fractured rock aquifer	Kilroy (1992)	Nevada, USA	GR
	Larocque et al. (1988)		
	Desbarats et al. (1999)	British Columbia, Canada	R&C
	Lee and Lee (2000)	Wonju, South Korea	Q&R, CLK
	Bernard and Delay (2008)	Poitiers, France	Q&R
	Burbey (2010)	Virginia, USA	LR
	Cutillo and Bredehoeft (2011)	California and Nevada, USA	LR
	Fileccia (2011)	Otavi, Namibia	R&C
	Burbey et al. (2012)	Virginia, USA	Assumed value
Aquitard	Timms and Acworth (2005)	New South Wales, Australia	LR
	Larroque et al. (2013)	Bordeaux, France	LR
	Smith et al. (2013)	Saskatchewan, Canada	BAR
	Smerdon et al. (2014)	Great Artesian Basin, Australia	BAR
	David et al. (2017)	New South Wales, Australia	BAR, LR
	Rau et al. (2018)	New South Wales, Australia	ACW

A&B = Acworth and Brain (2008); ACW = Acworth et al. (2016); AM = analytical modeling; BAR = Barr et al. (2000); DMA = departure from moving average; D&R = Davis and Rasmussen (1993); GR = graphical; LR = linear regression; NM = numerical modeling; Q&R = Quilty and Roeloffs (1991); RAH = Rahi (2010); CLK = Clark (1967); R&C = Rasmussen and Crawford (1997).

In the present study, a range of existing approaches were implemented in order to estimate three key variables: (1) the degree of aquifer confinement; (2) barometric efficiency; and (3) specific storage. For the assessment of aquifer confinement, two methods were compared: Fourier analysis and regression deconvolution. For the estimation of BE, three frequency domain and five time domain methods were compared. Specific storage values were subsequently calculated using the Jacob (1940) solution

from estimated BE values while incorporating historical estimates of effective porosity derived from downhole resistivity data.

Theoretical Background

Butler et al. (2011) described the physical processes involved in the transmission of barometric pressure loading from the ground surface (1) to a confined aquifer

and (2) to an unconfined aquifer. The same concepts were depicted visually by He et al. (2016). The descriptions provided by Butler et al. (2011) are paraphrased as follows.

In confined aquifers, barometric pressure loading at the land surface is transmitted downward from grain to grain to the interface between the aquifer and an overlying confining layer. Below the confining layer, part of the load is accommodated by the aquifer pore water and part is accommodated by the aquifer matrix. In contrast, the entire load is accommodated by the water column in a groundwater well open to the atmosphere. The resulting pressure difference at the well screen induces water flow between the aquifer and the well, leading to the commonly observed inverse relationship between barometric pressure and groundwater levels in wells open to the atmosphere. The magnitude of the groundwater pressure reduction primarily depends on how the imposed load is shared between the aquifer pore water and the aquifer matrix, although the properties of the aquifer and overlying units and the characteristics of the well (e.g., well diameter and degree of well development) can also be significant.

In unconfined aquifers, groundwater level responses are primarily the result of the downward propagation of air pressure through pores in the vadose zone. In areas featuring shallow water tables, this propagation can occur so quickly that pressure differences between the well and the aquifer are negligible. Consequently, barometric pressure loading may not induce a pressure difference between the aquifer and the well. Alternatively, in areas featuring deep water tables or low pneumatic diffusivity (i.e., low porosity), the propagation of air pressures may be delayed, thereby causing a delay before barometric pressure loading effects may be observed. Thick and/or low permeability unsaturated zones can result in considerable attenuation and phase shift of periodic signals, resulting in time-delayed barometric responses (Fischer 1992).

A number of metrics have been proposed to characterize groundwater responses to barometric pressure fluctuations. The metric of tidal efficiency, first proposed in hydrogeological literature by Jacob (1940), describes the magnitude of the groundwater response. Ferris (1952) later proposed the alternative term “amplitude factor” when describing the same concept. This concept has since become widely known instead as BE (Rasmussen 2005a), whereas “tidal efficiency” is now almost exclusively used to refer to aquifer responses to ocean tides (in the horizontal plane, rather than the vertical plane) (Rasmussen 2005b). When an external stress is imposed on an aquifer, the stress is partitioned between (1) the rock or sediment matrix and (2) the pore water contained within. BE represents the proportion of imposed stress that is accommodated by the rock or sediment matrix (Domenico and Schwartz 1990). A BE value of zero will result in no observable response, as all of the imposed stress is accommodated by the pore water. Conversely, a BE value of one indicates zero loss of pressure during transmission, as all

of the imposed stress is accommodated by the rock or sediment matrix.

A complementary concept referred to as “loading efficiency” (γ) was first proposed by van der Kamp and Gale (1983). This metric can be calculated as $\gamma = 1 - BE$; therefore it represents the proportion of imposed stress that is accommodated by the pore water. For uniaxial strain under undrained conditions, loading efficiency is equivalent to Skempton’s coefficient (B ; Skempton 1954), which is commonly used in geotechnical studies (Wang 2000). Specifically, for porous media featuring incompressible grains, $B = \gamma$ while for media featuring compressible grains, $B \approx 3\gamma$. To avoid confusion of terminology in the present study, discussion of these alternative metrics is avoided and the concept of BE is used exclusively in the present study.

BE is calculated using the ratio of (1) the instantaneous change in groundwater pressure (dw) to (2) a change in barometric pressure at the ground surface (db). In practice, this change is approximated using temporal finite differences, which are typically evaluated over an hourly period:

$$BE = 1 - \frac{dw}{db} \approx 1 - \frac{\Delta w}{\Delta b} \quad (1)$$

The concept of BE can be used to quantify the relative contributions of matrix compressibility (C_M) and pore water compressibility (C_W ; $= 4.58 \times 10^{-10}/\text{Pa}$ for freshwater) to observed groundwater responses to barometric pressure fluctuations. This relationship was first described as a function of C_M , C_W and effective porosity (θ_E) by Jacob (1940) as:

$$BE = 1 - \frac{C_M}{C_M + \theta_E C_W} \quad (2)$$

When BE is well-characterized (e.g., using one of the approaches described in the subsequent Methods section), this equation can instead be solved for matrix compressibility:

$$C_M = \frac{\theta_E C_W (1 - BE)}{BE} \quad (3)$$

Equation 3 can be used to estimate the physically reasonable range of matrix compressibility values for specified effective porosity and BE values (Figure 1). BE values range from zero (left) to one (right), while effective porosity values range from 1% (yellow) to 33% (dark blue). For the range of possible effective porosity values (i.e., 1-33%), minimum matrix compressibility values occur at $\leq 10^{-14}/\text{Pa}$ (e.g., marble), at which barometric pressure fluctuations are entirely accommodated by the rock matrix (i.e., $BE = 1.0$). Conversely, maximum matrix compressibility values occur at $\geq 10^{-6}/\text{Pa}$ (e.g., unconsolidated clay), at which barometric pressure fluctuations are entirely accommodated by the pore water (i.e., $BE = 0.0$). Matrix compressibility values at which the stress balance is shared equally between the matrix and the pore water

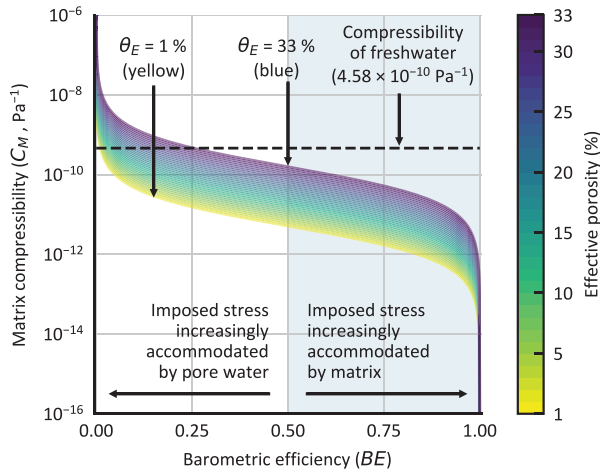


Figure 1. Theoretical range of matrix compressibility values (colored sigmoidal area) calculated using Equation 3 as a function of barometric efficiency values ranging from zero (left) to one (right) and effective porosity values ranging from 1% (yellow) to 33% (dark blue). Also shown for reference is the compressibility of freshwater (4.58×10^{-10} Pa⁻¹; dashed black line).

(i.e., BE = 0.5) can be identified. Specifically, C_M values will range from $\approx 10^{-11.3}$ Pa (for $\theta_E = 1\%$) to $\approx 10^{-9.6}$ Pa (for $\theta_E = 33\%$).

Most metrics used to characterize groundwater responses to barometric pressure fluctuations assume that responses are instantaneous. Furbish (1991) and Rasmussen and Crawford (1997) were the first to consider delayed groundwater responses. They used regression deconvolution to estimate responses at a finite number of specified time lags. In the present study, these responses are termed impulse response functions (IRFs) for clarity. Various parametric functions can be used to identify hydrogeological conditions from IRF results, including confined aquifer responses (Rasmussen and Crawford 1997), unconfined aquifer responses (Weeks 1979), borehole storage effects (Hvorslev 1951; Furbish 1991), and aquitard leakage (Butler et al. 2011). Rasmussen and Crawford (1997) calculated cumulative sums of IRF values to estimate what they termed barometric response functions (BRFs). In the present study, IRFs were used to estimate aquifer confinement status.

Methods

Characterization of Aquifer Confinement

Two methods were used to characterize aquifer confinement. The first method involved the use of Fourier analysis to convert groundwater hydrograph data from the time domain to the frequency domain. From these results, the amplitude observed at a selected Earth tide component frequency was used as a semiquantitative measure of the degree of aquifer confinement. The second method involved the use of regression deconvolution to estimate groundwater responses as functions of time delay. The

Table 2
Five Major Components of the Earth Tide Potential (Munk and MacDonald 1960)

Component	Description	Period (Days)	Frequency (cpd)
O_1	Principal lunar	1.0758	0.9295
K_1	Lunar-solar	0.9973	1.0027
N_2	Lunar elliptic	0.5274	1.8960
M_2	Principal lunar	0.5175	1.9323
S_2	Principal solar	0.5000	2.0000

shape of these response functions was used to estimate aquifer confinement status.

Fourier Analysis

The discrete Fourier transform (DFT) can be used to decompose a given time series of observations (such as groundwater pressure head data) into a linear sum of a finite number of sinusoidal functions (Kanasewich 1981). The results of the DFT are typically summarized using an amplitude spectrum, which presents the amplitude at each calculated frequency. The maximum frequency that can be calculated using the Fourier transform is half that of the sampling frequency, as stated by the Nyquist-Shannon sampling theorem (Kanasewich 1981). For example, if observations are recorded at hourly intervals (i.e., 24 cycles per day) then the maximum frequency that can be observed when using a Fourier transform is 12 cycles per day (cpd). The resolution of DFT results is a nonlinear function of sampling duration. Specifically, the DFT output bin size is inversely proportional to sampling duration; that is, the longer the duration of sampling, the smaller the output bin size. However, because this relationship is nonlinear, cumulative improvements in DFT resolution decrease with sampling duration. For example, if sampling at a frequency of 1 cpd then DFT resolutions of 0.1, 0.01, and 10^{-3} cpd can be achieved using time series lengths of 10 d, 100 d, and ~ 2.7 years respectively. Conversely, to achieve a DFT resolution of 10^{-4} cpd or less would require a sampling duration of more than 27 years.

Gravitational forces exerted on the Earth by the combined motions of the sun and moon are known as Earth tides. These result in small latitudinal and longitudinal strains within the solid crust of the Earth. The combined tidal gravitational potential of the sun and moon can be described using a finite set of tidal components (Doodson and Warburg 1941). Each component can be represented using a harmonic (i.e., periodic) function that has a unique frequency, amplitude and phase. Five tidal components typically account for about 95% of the Earth tide potential (Cuttillo and Bredehoeft 2011); these are listed in Table 2.

When using DFT results to estimate the amplitude of a given Earth tide component, the input time series length can be adjusted (using a least squares optimization

algorithm) to position a bin edge as close as possible to a frequency of interest. For a given input time series, the optimal length will typically be less than the total length, and more than one optimal length may exist. In the present study, bin edges were optimized to match the frequencies of the M_2 and S_2 Earth tide components to a precision of four decimal places.

Fourier transform results are subject to interference between various frequencies, commonly known as spectral leakage. For example, the one cpd signal may affect amplitude estimates at other frequencies that are multiples of one; for example, at two and three cpd. For this reason, frequency domain filtering is typically used to remove or minimize the adverse effects of spectral leakage. In the present study, a Hann window (aka Hanning window; Kanasewich 1981) was applied to all input datasets, as used in previous studies (e.g., Acworth et al. 2016).

Frequency domain analysis methods were used to calculate amplitudes of three frequencies (i.e., 1.0027, 1.9323, and 2.0000 cpd) corresponding to selected Earth tide harmonic components (i.e., K_1 , M_2 , and S_2 respectively) (Melchior 1983). These were calculated using three separate input data types. Amplitudes of the S_2 Earth tide harmonic component were calculated from observations of atmospheric barometric pressure and groundwater pressure heads, as well as from theoretical Earth tide potentials. Amplitudes of the M_2 Earth tide harmonic component were calculated from observations of groundwater pressure head and from theoretical Earth tide potentials. All datasets were subsequently used as inputs to the Acworth et al. (2016) method of BE calculation.

Regression Deconvolution

Following earlier theoretical development by Furbish (1991), Rasmussen and Crawford (1997) proposed the use of a regression deconvolution approach to characterize groundwater pressure responses to barometric fluctuations. Specifically, incremental changes in groundwater pressure at time t [i.e., $\Delta w(t)$, which is equal to $w(t) - w(t - \Delta t)$] can be calculated as the convolution of changes in barometric pressure prior to time t up to a maximum time lag [i.e., $\Delta b(t) = b(t) - b(t - i\Delta t)$, where i = the number of time lags] with an impulse response function [IRF(τ)]. IRF values were calculated by minimizing the sum of squared differences between estimated (via convolution) and observed groundwater pressure responses. In the present study, least squares optimization was undertaken using the Levenberg-Marquardt optimization algorithm (Levenberg 1944; Marquardt 1963), implemented as the *curve_fit* function in the Python language. The cumulative response function at a given time lag τ [i.e., termed the “barometric response function”; BRF(τ)] was calculated as the cumulative sum of IRF values up to the time lag τ of interest. The regression deconvolution approach derived by Rasmussen and Crawford (1997) has been applied in seven published studies (Table 1).

Rasmussen and Crawford (1997) presented three end members by which to interpret the dynamics observed in estimated BRF values. A parametric model was proposed

for the interpretation of each end member. First, BRF values that are constant with respect to time lag size indicate confined conditions. Second, BRF values that decrease exponentially with respect to time lag size indicate unconfined conditions. Third, BRF values that increase logarithmically with respect to time lag size indicate borehole storage and/or well skin effects.

BE Estimation

Frequency domain and time domain methods of BE estimation are now described briefly.

Frequency Domain Approaches

Frequency domain methods involve decomposing an observed time series into a linear sum of harmonic (i.e., periodic) components, each of which is unique to a specific frequency. Various basis functions can be used to represent harmonic components, including wavelets (e.g., Dong et al. 2015; Acworth et al. 2016), but the most commonly used are sinusoidal functions. The decomposition of a time series into sinusoidal functions is commonly undertaken using Fourier transform methods (Kanasewich 1981), such as the DFT (typically implemented as the fast Fourier transform). Three frequency domain approaches were implemented in the present study, and are described as follows.

Quilty and Roeloffs (1991) Method

Following earlier work by Galloway and Rojstaczer (1988), Quilty and Roeloffs (1991) derived a solution by which to estimate frequency-dependent BE values from cross-spectral density (CSD) and power spectral density (PSD) analyses of time series data. Bernard and Delay (2008) later independently derived an identical solution based on works by Padilla and Pulido-Bosch (1995) and Larocque et al. (1988). Specifically, for a given frequency of interest, BE can be calculated as the ratio of (1) the CSD of a vector of time series of barometric (**b**) and groundwater (**w**) pressure observations to (2) the square root of the PSD of **b**. Variations in BE values calculated as functions of frequency were examined by Rojstaczer (1988), Lee and Lee (2000), Hussein et al. (2013), and Odling et al. (2015). In the present study CSD and PSD values were estimated via the calculation of DFTs using Welch’s method (Welch 1967). Specifically, amplitude values calculated via DFTs were compared at frequencies corresponding to the diurnal (i.e., K_1 ; ≈ 1.0 cpd) and semi-diurnal (i.e., S_2 ; 2.0 cpd) Earth tide components. These frequencies were selected as they were consistently identified at all 10 wells as frequencies at which amplitudes (calculated using the DFT) were in excess of noise.

Acworth et al. (2016) Method

Acworth and Brain (2008) calculated BE values using ratios of Fourier transform-derived amplitudes of selected Earth tide components observed in groundwater and barometric pressure data. Specifically, BE values were either calculated using the ratio of the amplitudes

of K_1 or S_2 tidal components. However, Acworth and Brain (and previously, Merritt 2004) did note that both K_1 and S_2 tidal components are both typically contaminated by other diurnal and semi-diurnal processes, such as evapotranspiration and/or groundwater extraction. Acworth and Brain provided a correction to the method by incorporating the amplitude of the M_2 tidal component, which is only observed in confined and semiconfined aquifers.

Acworth et al. (2016) subsequently developed a new method which used the Harmonic Addition Theorem (Arfken and Weber 2005) to disentangle the groundwater response to influences from both barometric pressure fluctuations and Earth tides. This approach was the first to establish the relative influence of Earth tides on groundwater pressures by quantifying the amplitudes of the M_2 tidal components present in both (1) groundwater pressure and (2) synthetic Earth tide datasets. The relative Earth tide magnitude should be the same at the S_2 frequency and can subsequently be removed to reveal the response to barometric pressure fluctuations. In the present study, amplitudes and phases of signals at selected Earth tide component frequencies (i.e., M_2 and S_2) were estimated using DFTs. Amplitude and phase information for barometric and groundwater pressure signals were derived from field data. Phase information for the M_2 component of the theoretical Earth tide was calculated from synthetic Earth tide outputs produced using the Python language library *PyGTide* (Rau 2018) over the same time period and at the same well locations as the acquired field data.

Time Domain Approaches

Time domain methods are based on relating incremental changes in barometric pressure to incremental changes in groundwater pressure. Five time domain approaches were implemented in the present study, and are described as follows.

Average-of-Ratios and Median-of-Ratios Methods

The average-of-ratios method involves calculating the ratio of incremental change in groundwater pressure (Δw) to incremental change in barometric pressure (Δb) at each observation time. BE can then be calculated as the mean value of $\Delta w/\Delta b$ over the total time of observations (i.e., BE_{AOR}). Similarly, using the median-of-ratios method, BE can be calculated as the median value of $\Delta w/\Delta b$ over the total time of observations (i.e., BE_{MOR}) (Gonthier 2007). As with the general use of the mean to summarize a statistical population, the average-of-ratios method is particularly sensitive to large $\Delta w/\Delta b$ values (i.e., outliers). Consequently, the average-of-ratios method was not considered to be a robust method of BE estimation.

Linear Regression Method

Ordinary least squares regression may be used to estimate the parameters of a linear function that describes a vector containing incremental changes in groundwater

pressure (Δw) as a function of a vector of incremental changes in barometric pressure (Δb). BE can then be calculated as the slope of the estimated linear function. Linear regression was first used to estimate BE values by Robinson and Bell (1971) and was subsequently applied in 18 published studies (Table 1).

Clark (1967) Method

Clark (1967) proposed a method of BE estimation based on the calculation of cumulative sums for both Δb and Δw . For Δb , the cumulative sum of absolute changes in barometric pressure (i.e., $\Sigma \Delta b$) is calculated, with the exception of zero-valued Δb values, which are omitted. Conversely, for Δw a sign test is applied in order to determine whether the absolute value of Δw at a given time is either added or subtracted from the cumulative sum. Specifically, at each time step the signs of Δb and Δw are compared. If Δb and Δw are both positive, or if Δb and Δw are both negative, then the absolute value of Δw is added to the cumulative sum of Δw values (i.e., $\Sigma \Delta w$). Alternatively, if the signs of Δb and Δw are not in agreement then the absolute value of Δw is subtracted from $\Sigma \Delta w$. In addition, for time steps at which Δb is zero-valued, Δw values are excluded. BE is then calculated as the ratio of the cumulative sums calculated; that is, $BE_{CLK} = \Sigma \Delta w / \Sigma \Delta b$. The Clark method was applied in seven published studies (Table 1). Gonthier (2007) compared the Clark method to the average-of-ratios, median-of-ratios and linear regression methods when estimating BE values at 45 wells at Air Force Plant 6 in Marietta, Georgia, USA. Davis and Rasmussen (1993) proposed a modification to the Clark method which accounted for the effect of long-term trends.

Rahi (2010) Method

Rahi (2010) proposed an alternative version of the Clark method which included tests of both the signs and magnitudes of pressure changes. Specifically, the cumulative sums of changes in barometric pressure ($\Sigma \Delta b$) and groundwater pressure ($\Sigma \Delta w$) are only modified when (1) the signs of Δb and Δw are in agreement and (2) the absolute value of Δw is less than the absolute value of Δb . BE is then calculated as the ratio of cumulative sums; that is, $BE_{RAH} = \Sigma \Delta w / \Sigma \Delta b$. Applications of the Rahi method have been limited to three published studies.

Specific Storage Estimation

While BE values can provide insight into aquifer lithology (e.g., Palciauskas and Domenico 1989; Hobbs and Fourie 2000), they are most valuable as an intermediate property that can be used to estimate matrix compressibility (via Equation 3) and specific storage (via Equation 4). Methods of interpreting elastic storage properties from groundwater responses to barometric pressure fluctuations were first proposed by Cooper et al. (1965), Bredehoeft (1967), and Clark (1967). Jacob (1940) first proposed that specific storage could be calculated as a

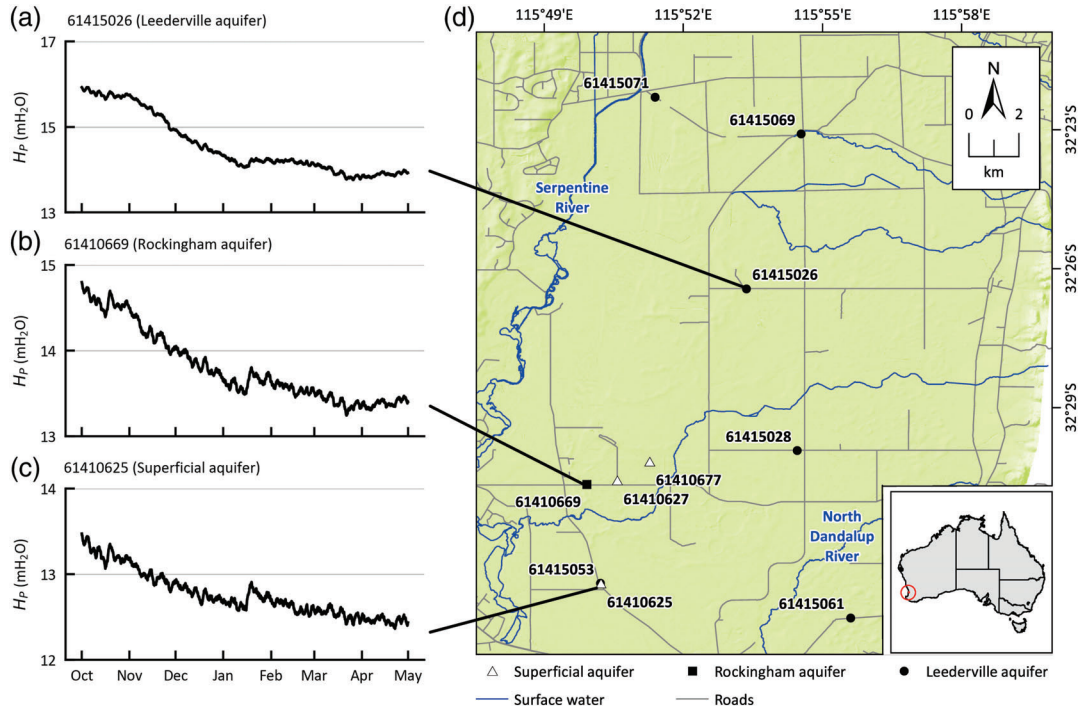


Figure 2. (a-c) Groundwater pressure head (w) observations from three selected wells recorded at an hourly frequency over the period October 2017 to May 2018. (d) Spatial distribution of 10 groundwater pressure loggers installed in the Peel region of southwestern Western Australia. A barometric pressure logger was also installed at well number 61415026.

function of BE:

$$S_S = \frac{\rho_W g \theta_E C_W}{BE} \quad (4)$$

where ρ_W = groundwater density (M/L^3) and g = the gravitational constant (L/T^2). While approximate values can generally be assumed for three variables (i.e., $\rho_W \cong 1000 \text{ kg/m}^3$, $\cong 9.81 \text{ m/s}^2$, and $C_W \cong 4.58 \times 10^{-10}/\text{Pa}$), site-specific (or at least, lithology-specific) characterization of effective porosity is required. Equation 4 accounts for water compressibility explicitly, while matrix compressibility is included implicitly via BE. Grain compressibility is excluded from Equation 4, which requires the assumption that grains are incompressible. For unconsolidated sedimentary aquifers, a comprehensive characterization of specific storage that does account for grain compressibility (van der Kamp and Gale 1983; Green and Wang 1990) should instead be used. This can involve the use of cross-borehole seismic surveys to estimate the additional poroelastic parameters required (Rau et al. 2018). Conversely, for aquifers hosted in consolidated rocks (such as those assessed in the present study), the assumption of grain incompressibility can be justified.

Study Area Description

The Peel region study area is located south of Perth in Western Australia and covers an area of 440 km^2 (Figure 2d). The region is bounded by the Darling Scarp in the east (not shown), by the Serpentine River in the north and west, and by the Dandalup rivers (including

the North Dandalup River) in the south. A number of perennial streams originate from elevated areas in the east and flow westward through the region toward the coast. Ephemeral streams originate in coastal plain areas closer to the coast. The Peel area features a Mediterranean climate of hot, dry summers and mild, wet winters. The long-term mean annual precipitation is 860 mm, with approximately 90% of rainfall occurring between April and October (i.e., Southern Hemisphere winter), and a mean annual potential evaporation of 1800 mm (Davidson and Yu 2008).

Potable groundwater resources occur in various aquifers across the region. The surficial Superficial aquifer is extensive across the Peel area, with a sedimentary composition that ranges from clayey sediments adjacent to the Darling Scarp in the east, to sandy sediments in the central coastal plain area, to limestone rocks along the coast in the west. The saturated thickness of the Superficial aquifer typically ranges from 20 to 50 m, with hydraulic properties varying considerably depending on lithology. The Rockingham aquifer underlies the Superficial aquifer and consists of medium to coarse sand, with a mean hydraulic conductivity of approximately 20 m/d. Occurring at greater depths is the Leederville Formation, a major confined aquifer that is present across the entire Perth region. The Leederville aquifer consists of discontinuous interbedded sandstones, siltstones and shales ranging from 50 to 500 m in total thickness. The hydraulic conductivity of the sandstone members of the Leederville aquifer is typically 10 m/d (Davidson and Yu 2008).

Groundwater in the study area is currently used for a broad range of applications, including agricultural activities (e.g., irrigation, horticulture, turf production, and livestock watering), as well as extractive industries (including sand mining). The total volume of groundwater extraction in 2016 was estimated at 14.3 GL from Superficial aquifers and 6.8 GL from Leederville aquifers. These both represented historical maxima, having increased from rates of less than 2 GL per annum prior to 1987 for both aquifer types.

Groundwater pressure data were obtained at 10 sites located across the study site. Data were recorded at hourly intervals using nonvented In-Situ LevelTROLL™ data loggers over a period of 7 months (i.e., October 2017 to April 2018) (e.g., Figure 2a-2c). These data were not converted to hydraulic head, nor corrected for barometric fluctuations (as is commonly undertaken for groundwater pressure data). Barometric pressure observations were recorded at hourly intervals using an In-Situ BaroTROLL™ barometric pressure logger suspended inside the casing of groundwater well 61,415,026. Hydrograph data were visually inspected to ensure the effects of localized groundwater extraction were not present. Well construction details were reviewed to ensure that recorded groundwater pressure data remained consistently above top-of-screen elevations.

The primary temporal trend consistently observed in groundwater pressure hydrographs was a decline in pressure during the November-February period (i.e., southern hemisphere summer), which featured few rainfall events. Declining trends observed in unconfined wells were generally linear, whereas declining trends observed at confined wells were generally parabolic (i.e., concave). Responses to a single large (i.e., >100 mm) rainfall event in mid-January 2018 were observed in most well hydrographs. Although this resulted in mechanical loading (van der Kamp and Schmidt 2017) at the ground surface for a limited period of time, this event was not periodic and therefore it did not affect the results of the present study.

Time series data were processed prior to their inclusion in BE analyses according to the following workflow. Incremental differences between barometric and groundwater pressure observations (i.e., Δb and Δw respectively) were calculated over hourly intervals using backward differences. For time domain analyses, influences from Earth tide components (which feature frequencies of 0.9-2.0 cpd) were removed from each time series by use of digital filtering. Specifically, a first-order Butterworth low pass filter (Rabiner and Gold 1975) was used to exclude frequencies greater than 0.8 cpd (e.g., Geldon et al. 1997). Filtering was not undertaken prior to frequency domain or regression deconvolution analyses in order to avoid introducing artifacts.

Results

For all BE estimation methods, results are presented for a subset of three wells that represent each of the three

Peel region aquifers assessed (i.e., Superficial, Rockingham, and Leederville). Fourier analysis and regression deconvolution were used to estimate confinement status. The former method used the amplitude of the M_2 Earth tide component to estimate the degree of aquifer confinement. The latter method estimated confinement status by evaluating the time delay between groundwater responses and barometric pressure fluctuations. For wells identified as being semiconfined or confined, a range of frequency and time domain methods were subsequently used to estimate instantaneous BE values. BE values were then used to estimate specific storage values.

Characterization of Aquifer Confinement

Fourier Analysis

Amplitude spectra for a subset of three wells representative of the three Peel region aquifers (i.e., Superficial, Rockingham, and Leederville) are presented in Figure 3b-3d. The amplitude spectrum of the theoretical Earth tide at the study site over the period of groundwater monitoring is also presented for comparison (Figure 3a). The degree of well confinement was assessed through visual inspection of amplitude spectra calculated using DFTs. Relatively large magnitude responses to the K_1 and S_2 Earth tide components were observed at the majority of wells. Conversely, responses to the O_1 or N_2 Earth tide components were not observed at any wells. Relatively large M_2 amplitudes (i.e., in excess of noise) were considered to be robust indicators of semiconfined or confined conditions (Rahi and Halihan 2013). Observed M_2 amplitudes were <0.5 mm at Superficial aquifer wells (e.g., Figure 3c), thereby confirming unconfined conditions. All three Superficial aquifer wells were subsequently excluded from the calculation of specific storage values. M_2 amplitudes were greater than 1.0 mm at all confined and semiconfined wells (e.g., Figure 3a and 3b), with maximum values (i.e., >3.9 mm) observed at wells 61415028 and 61415053.

Regression Deconvolution

The regression deconvolution approach to BE estimation required the specification of a finite number of uniformly distributed lag times, up to a maximum lag time. Past implementations of the approach used a priori or arbitrarily-defined estimates of maximum lag times (e.g., Butler et al. 2011). In the present study, IRFs estimated using regression deconvolution were instead used to identify the maximum time lag for which nonzero correlations were observed. Regression deconvolution results for a subset of three wells representative of the three Peel region aquifers (Superficial, Rockingham, and Leederville) are presented in Figure 3e-3i.

A maximum time lag length of ≤ 6 h was consistently identified from estimated IRF values. Impulse response function values at time lags greater than 6 h oscillated around a zero mean value and represented random noise rather than actual correlation. For the majority of wells, IRF values decreased logarithmically and rapidly to an

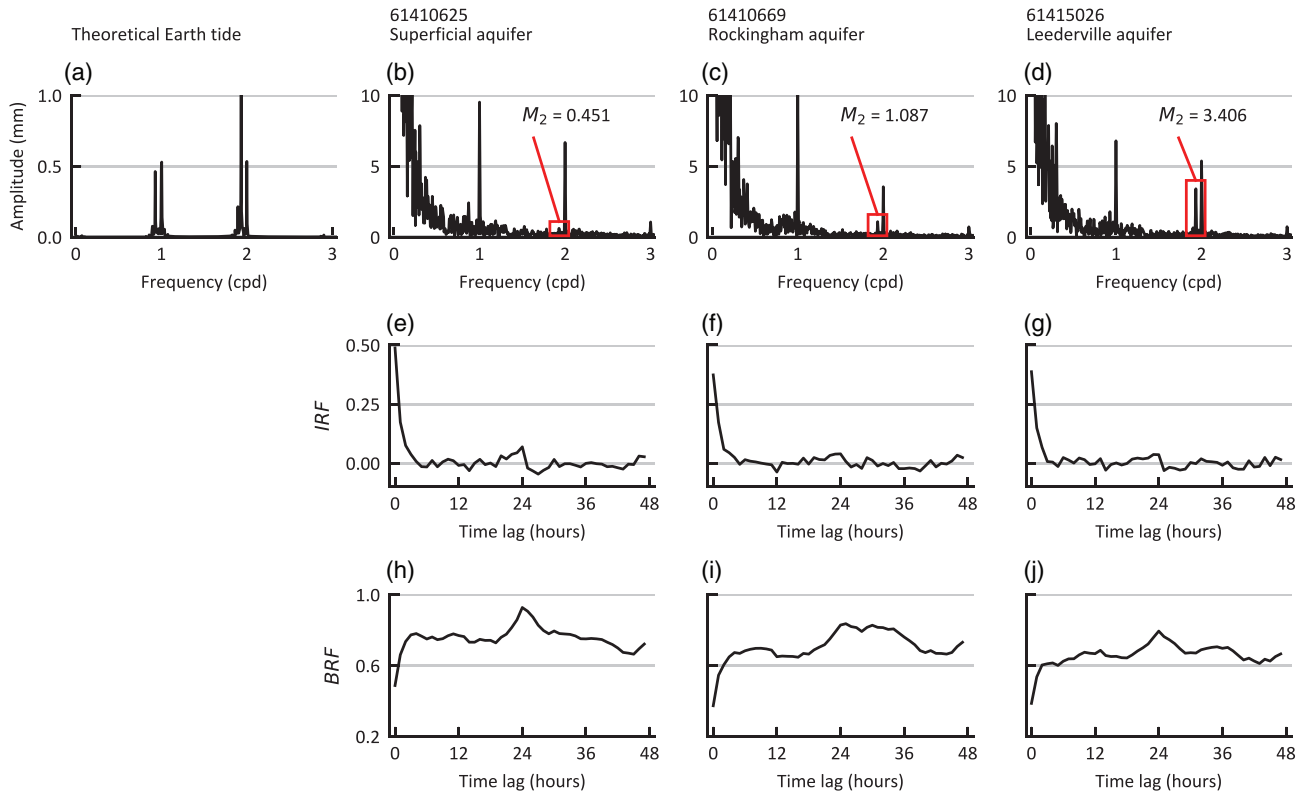


Figure 3. Amplitude spectra of (a) the theoretical Earth tide and (b-d) groundwater pressure head data computed from Fourier analysis. (e-g) Impulse response functions (IRFs) estimated via regression deconvolution. (h-j) Barometric response functions (BRFs) calculated as cumulative sums of respective IRF values. IRF and BRF values were plotted as functions of lag time length (in hours), based on data collected from three groundwater wells in the Peel area of Western Australia over the period October 2017-April 2018.

asymptotic near-zero value. These dynamics are consistent with (1) minimal borehole storage and/or well skin effects at early times (i.e., time lags of ≤ 6 h) and (2) confined aquifer responses at later times (i.e., time lags of ≤ 18 h).

BRF values increased rapidly to reach asymptotic values after time lags of ≤ 6 h at all wells. Asymptotic values were relatively consistent at most wells for time lags of 6-18 h, except for well 61,415,069. Maximum BRF values consistently occurred at a time lag of 24 h, at both confined and unconfined wells. This anomaly is examined in further detail in the discussion of aquifer confinement results.

BE Estimation

Frequency Domain Approaches

Three frequency domain methods of estimating BE are compared in Figure 4a-4c. These were two Quilty and Roeloffs (1991) solutions (based on either the K_1 or S_2 Earth tide components) and the Acworth et al. (2016) solution. Of the three frequency domain methods tested, the Quilty and Roeloffs (Q&R) method based on the S_2 tide was found to be the most robust. At the majority of confined wells, BE values estimated using the Q&R K_1 solution were greater than unity. These indicated the presence of additional processes featuring a frequency of approximately one cpd; for

example, evapotranspiration and/or extraction. At wells featuring M_2 Earth tide component amplitudes greater than 1 mm, BE values estimated using the Acworth et al. (2016) solution were larger than those estimated using the Q&R S_2 method. This was consistent with the effect of scaling the estimated BE value by the ratio of M_2 Earth tidal components in barometric and groundwater pressure observations (Acworth et al. 2016).

Time Domain Approaches

Four time domain methods of estimating BE are compared in Figure 4d-4f. These were the linear regression, median-of-ratios, Clark, and Rahi methods. The average-of-ratios method was excluded due to its sensitivity to outliers. In particular, a large, abrupt increase in groundwater pressure resulting from a single large magnitude rainfall event in mid-January 2018 caused spurious results when applying the average-of-ratios method. The Rahi method consistently underestimated BE values in comparison to the other three time domain methods tested. In terms of the length of sampling duration, BE values estimated using the linear regression, median-of-ratios and Clark methods typically converged after 4 months. In order to assess whether barometric responses were nonstationary (i.e., time period-dependent), time domain BE values were also estimated using 4-month-long moving windows over the October 2017-April 2018 sampling

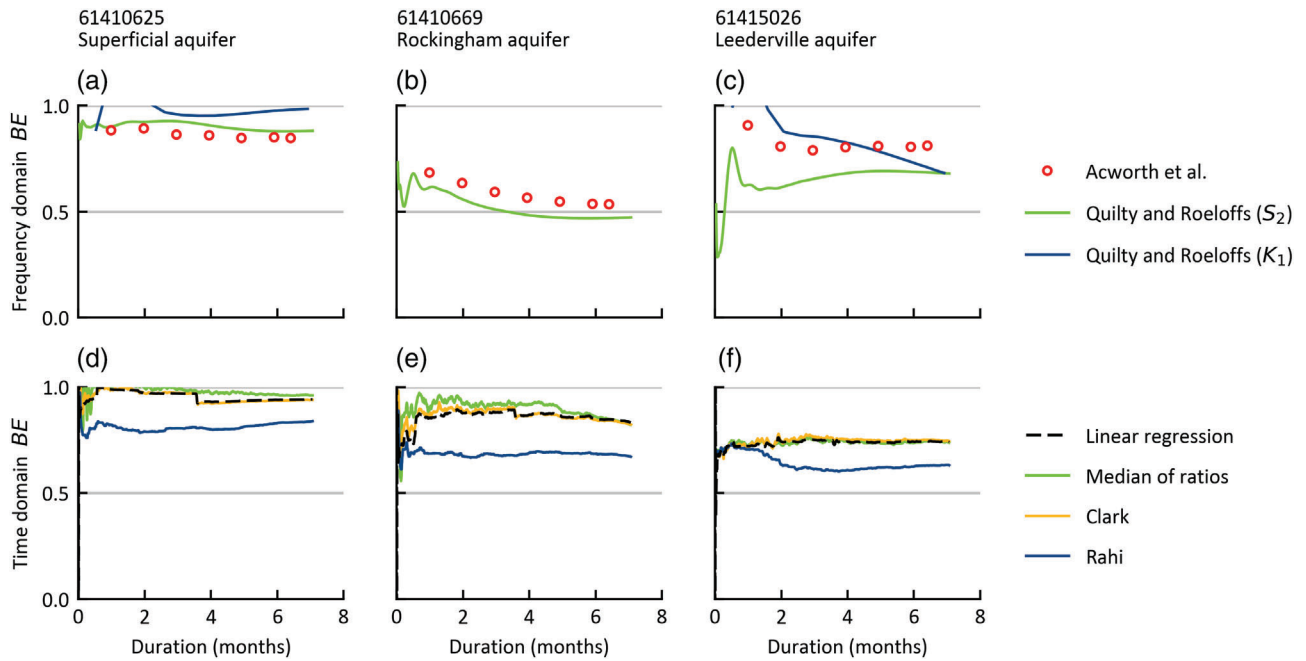


Figure 4. Instantaneous barometric efficiency (BE) estimates derived using (a-c) frequency domain and (d-f) time domain approaches. All results are plotted as functions of input duration, based on data collected from three groundwater wells in the Peel area of Western Australia over the period October 2017-April 2018.

period. BE values were found to be stationary at most sampled wells, thereby confirming this assumption.

Specific Storage Estimation

All BE and specific storage estimates derived from time domain and frequency domain methods are summarized in Figure 5. For specific storage values estimated using Equation 4 (Figure 5b), Figure 5a porosity value of 16% was assumed for the Leederville aquifer. This value was based on interpretation of historical downhole resistivity data.

All but two estimated specific storage values ranged from 7×10^{-7} to $3 \times 10^{-6}/\text{m}$, none of which exceeded the physically plausible upper limit of $1.3 \times 10^{-5}/\text{m}$ proposed by Rau et al. (2018). Four dual-well historical pumping tests were previously undertaken in confined sandstone aquifers of the Leederville Formation. Specific storage values estimated from these tests ranged from 2×10^{-6} to $8 \times 10^{-6}/\text{m}$. Although consistently smaller in magnitude, BE-derived estimates of specific storage were therefore found to be order-of-magnitude consistent with historical pumping test results.

Discussion

Characterization of Aquifer Confinement

Amplitudes of the M_2 Earth tide component estimated from Fourier analysis were used to characterize aquifer confinement status. Observed variations in the amplitude of the M_2 tidal component at confined wells indicated the variability of confinement in confined aquifers. In the traditional binary paradigm of

confinement, aquifers are classified as either confined or unconfined. This is often a convenience required for numerical modeling purposes. In practice, confinement status varies continuously from fully unconfined (in the absence of confining unit) to fully confined (in the absence of leakage). The confinement status of many aquifers historically designated as confined will be, to some degree, semiconfined, due to a finite amount of leakage from adjacent aquitards. Moreover, the confinement status of an aquifer may change over time due to variations in water table elevation. Fourier analysis provides a robust means of comparing the spatial and temporal variability of confinement in an aquifer. For example, comparisons of amplitudes at frequencies other than one and two cycles per day may be used to investigate the spatial variability of aquitard thicknesses, including identifying areas of inter-aquifer leakage (e.g., Timms and Acworth 2005). Temporal variations in aquifer confinement may be assessed through the calculation of Earth tide responses using a fixed sampling duration that moves through time (McMillan et al. 2019).

Regression deconvolution was used to assess whether time lag-dependent groundwater responses to barometric fluctuations were present. Minor borehole storage effects were observed at all wells for time lags ≤ 6 h. This was consistent with known well dimensions, with internal well diameters ranging from 50 to 114 mm. Minimal borehole storage effects would be expected for such narrow diameter wells. Maximum BRF values were consistently observed at time lags of 24 h. This anomaly has been observed previously (Rasmussen and Crawford 1997; well FC-2F) but the source of this feature has not been identified. In the present study, a range

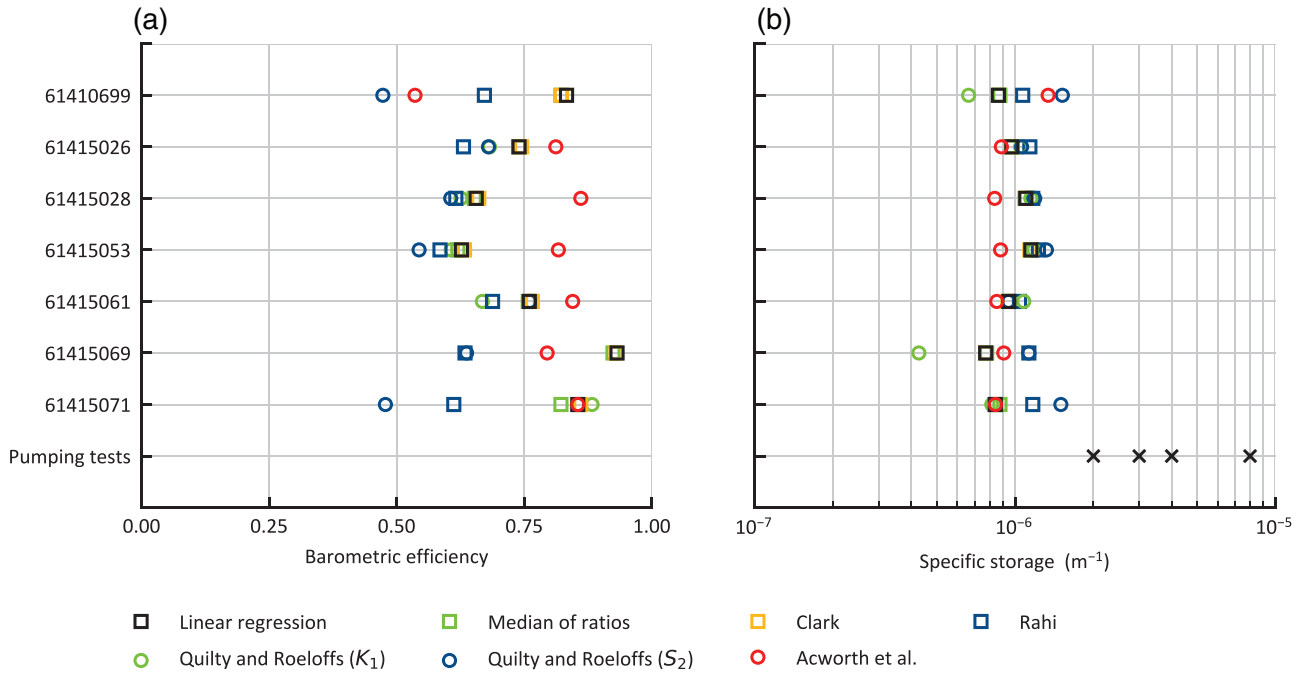


Figure 5. (a) Barometric efficiency values at seven groundwater wells in the Peel region of Western Australia calculated using various time and frequency domain methods. (b) Specific storage values calculated from barometric efficiency values using Equation 4. Also shown are specific storage estimates derived from four pumping tests conducted in the Leederville confined sandstone aquifer (black crosses).

of detrending and filtering methods were applied to both the barometric and groundwater pressure input data: linear or moving average trend removal, and Butterworth band stop and Hanning window filtering. None of these methods were successful in removing all anomalies observed at time lags of 24 h. These anomalies were interpreted as follows. For unconfined wells, anomalies were attributed to diurnal fluctuations in air temperature and evapotranspiration (Acworth et al. 2015). Since these processes (and therefore unconfined groundwater-level fluctuations) occur at a frequency of one cpd (with an associated harmonic at two cpd), frequency domain-based filtering methods cannot be used to correct for these effects. For confined wells, anomalies were attributed to Earth tide components. Specifically, according to the Harmonic addition theorem, where multiple periodic signals are present at a given frequency, the superposition of these signals will result in a new signal at the same frequency but featuring a unique amplitude and phase (Arfken and Weber 2005; Acworth et al. 2016; McMillan et al. 2019). For this reason, neither the subtraction of sinusoidal functions (in the time domain) nor band stop filtering (in the frequency domain) can remove confounding effects when two or more Earth tide components are present at a given frequency.

Fourier analysis was found to provide a more robust method of assessing aquifer confinement status than the regression deconvolution method. Specifically, Fourier analyses of Earth tide components with frequencies other than one and two cpd are robust against confounding

effects introduced by evapotranspiration and/or the superposition of multiple Earth tide components. In addition, M_2 tidal component amplitudes estimated by Fourier analysis provide a quantitative basis for relative comparisons of the degree of confinement over the spatial extent of an aquifer. For example, amplitude values may be used to identify locations where localized confinement occurs in a surficial aquifer, or locations where “windows” exist in an aquitard that otherwise confines an underlying aquifer (e.g., Timms and Acworth 2005).

BE Estimation

Instantaneous groundwater responses to barometric pressure fluctuations were estimated using three frequency domain methods, which varied in efficacy. The Quilty and Roeloffs method based on the K_1 Earth tide component was consistently a poor estimator. Estimated BE values were often in excess of unity and typically did not converge for up to 7 months sampling duration. In comparison, the Quilty and Roeloffs method based on the S_2 Earth tide component was generally the most robust estimator. Convergence upon a consistent BE value was achieved after 7 months’ sampling duration and good agreement with time domain results was generally observed. The Acworth et al. solution could only be computed using seven unique sampling duration lengths. This was due to the requirement that the amplitudes of the S_2 and M_2 Earth tide components be calculated simultaneously from Fourier analysis to a resolution of $\pm 10^{-4}$ cpd. In comparison, the Quilty and Roeloffs methods, which were based on comparisons of signals at a single frequency of interest, could

be calculated using a sampling duration of any given length.

Four time domain methods were used to estimate instantaneous groundwater responses to barometric pressure fluctuations. The average-of-ratios method was found to be a nonrobust estimator. The method was sensitive to outliers (specifically, a single large magnitude precipitation event in January 2018). The Rahi method was found to consistently underestimate BE values. In comparison, the results of the median-of-ratios and Clark methods were consistently in close agreement to those of the linear regression method.

It should be recognized that time domain methods may overestimate BE values when periodic but nonsinusoidal signals resulting from processes such as evapotranspiration are present (Acworth et al. 2015). Long-term trends such as hydrograph recession can be removed in the time domain using linear or moving average functions. Relatively high frequency (i.e., 1-2 cpd) signals resulting from processes such as Earth or ocean tides can be removed in the frequency domain using digital filtering. However, none of these methods are capable of removing nonsinusoidal signals such as evapotranspiration. The additional influence of evapotranspiration in a detrended, filtered hydrograph will result in overestimation of BE values. The presence of significant effects arising from evapotranspiration fluxes can be identified using the regression deconvolution approach as anomalies at time lags of 24 h.

While time domain methods are comparatively simple to implement, they may be confounded by processes such as evapotranspiration. This is also true for Quilty and Roeloffs methods based on the K_1 and S_2 Earth tide components (i.e., ≈ 1 and $= 2$ cpd, respectively). For these reasons, it is suggested that the Acworth et al. (2016) method is currently the most robust estimator of BE. By using the difference between M_2 tidal component amplitudes in groundwater observations and the theoretical Earth tide, the Acworth et al. solution can exclude the effects of confounding processes.

Specific Storage Estimation

Specific storage values calculated from BE estimates using Equation 4 (i.e., $> 4 \times 10^{-7}$ to $< 2 \times 10^{-6}/m$) were consistently smaller than values estimated from pumping tests (i.e., 2×10^{-6} to $8 \times 10^{-6}/m$). A potential explanation for this discrepancy is proposed as follows. All four pumping tests were interpreted using the Cooper and Jacob (1946) straight-line approximation of the Theis (1935) solution. These solutions assume that the tested aquifer is fully confined. In practice, it is possible that leakage from over- or underlying aquitards occurred during hydraulic testing. This would have resulted in overestimation of specific storage values. For example, Rau et al. (2018) recently identified a maximum physically plausible upper limit for specific storage values of approximately $1.3 \times 10^{-5}/m$. They attributed larger specific storage values typically estimated during past pumping test analyses to the failure to account for additional water sources, particularly leakage from overlying aquitards. The hypothesis

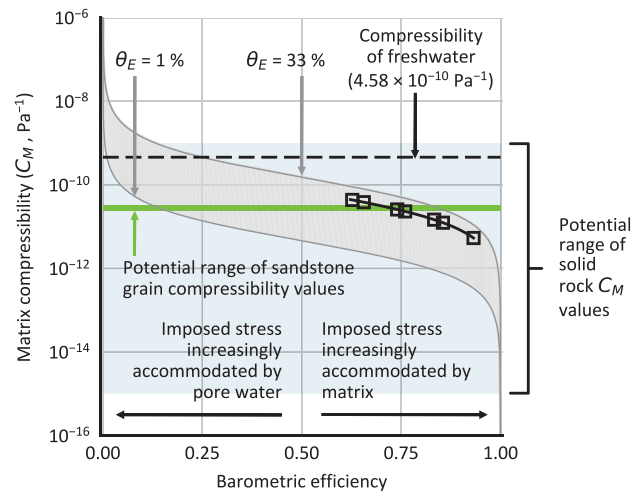


Figure 6. Matrix compressibility (C_M) values calculated from barometric efficiency values using Equation 3 (black open square symbols and solid black line). Barometric efficiency values were estimated using the time domain linear regression method at seven groundwater wells constructed in the Leederville aquifer. An effective porosity (θ_E) value of 16% (as derived from downhole resistivity data) was assumed for C_M calculations. The theoretical range of matrix compressibility values for effective porosity values ranging from 1 to 33% is indicated by the gray shaded sigmoidal area. The range of published C_M values for solid rocks (Domenico and Mifflin 1965) is indicated by the blue shaded area. The published range of grain compressibility values for sandstones (Detournay and Cheng 1993) is indicated by the thin green horizontal band.

that aquitard leakage occurs to the Leederville aquifer could be tested through reinterpretation of time-drawdown data recorded during hydraulic testing, including the use of diagnostic plots that include the first temporal derivative of drawdown (Renard et al. 2009).

The identification and acknowledgment of assumptions made when interpreting observed data is generally considered good practice, including in model regression (Saltelli et al. 2013; Peeters 2017). The methods of BE estimation tested in the present study required a range of assumptions. These included that imposed stresses were uniaxial (i.e., occurring in the vertical plane only) and the existence of undrained conditions. The latter assumes that there is insufficient time for water to flow in response to an imposed pressure fluctuation (Rau et al. 2018). The key assumption made when using the Jacob (1940) solution (Equation 4) to calculate specific storage values from BE estimates is that grains are incompressible. When grain compressibility is considerable, the assumption of grain incompressibility will lead to the overestimation of specific storage values (van der Kamp and Gale 1983).

To examine this assumption, the range of matrix compressibility (C_M) values calculated from BE estimates via Equation 3 (solid black line bounded by black open square symbols) is presented in Figure 6. For comparison purposes, also shown are: (1) the theoretical range of BE and C_M values for effective porosities of 1-33% (gray shaded sigmoidal area); (2) the potential range

of solid rock C_M values (blue shaded area); (3) the compressibility of freshwater (dashed black line); and (4) the known range of sandstone grain compressibilities (green horizontal band). The latter was derived from Detournay and Cheng (1993), who summarized a range of poroelastic parameters (including grain compressibility) derived from six sandstone samples (Rice and Cleary 1976; Yew and Jogi 1977; van der Kamp and Gale 1983). Collated sandstone grain compressibility values ranged from 2.4×10^{-11} to 3.2×10^{-11} /Pa (green dashed vertical lines). All estimated BE values were greater than 0.5, indicating that barometric pressure fluctuations at the seven groundwater wells were predominantly accommodated by the rock matrix. Five estimated BE values (ranging from 0.740 to 0.932) corresponded to matrix compressibility values that were less than the known range of sandstone grain compressibility. At these wells, the effects of grain compressibility on aquifer storage properties can be assumed to be negligible. Conversely, two estimated BE values (0.627 and 0.656) corresponded to matrix compressibility values that exceeded the known range of sandstone grain compressibility. In the absence of poroelastic parameter characterization (e.g., Rau et al. 2018) and site-specific testing of sandstone grain compressibility, the assumption of grain incompressibility at these two wells cannot be excluded. Past studies of sandstone samples indicated that the failure to account for grain compressibility can lead to overestimation of specific storage values by 5–12% (van der Kamp and Gale 1983).

Conclusions

This study compared, for the first time, two existing methods of confinement status estimation and eight existing methods of BE estimation. Comparisons were undertaken using field data from the Peel region of Western Australia. Three key conclusions were drawn from the results presented:

- 1 Fourier analysis provides a robust means of estimating aquifer confinement status. In comparison, response functions estimated using regression deconvolution can be confounded by the presence of evapotranspiration and/or other processes.
- 2 The Acworth et al. (2016) method of BE is currently the most robust estimator of BE. In comparison, time domain methods and the Quilty and Roeloffs frequency domain method can be confounded by the presence of evapotranspiration and/or the superposition of multiple tidal components at frequencies of one and two cpd.
- 3 The potential for grain compressibility to affect specific storage values calculated from BE estimates can be assessed through comparisons to equivalent matrix compressibility values. When estimated matrix compressibilities are larger than known ranges of grain compressibility (for a given rock or sediment type), corresponding specific storage values may be confounded

(specifically, overestimated) by the presence of grain compressibility.

The interpretation of groundwater responses to barometric pressure fluctuations provides an efficient, low-cost means of estimating (1) the relative degree of confinement, (2) the BE, and (3) the specific storage of semiconfined and confined aquifers. As the frequency and duration of observations required for these methods are minimal (e.g., a minimum of four observations per day over a 4-month period), in some cases BE estimation methods may enable additional insights to be derived from existing groundwater hydrograph data.

Acknowledgments

This research was undertaken as part of the Peel Integrated Water Initiative, a joint collaboration between CSIRO and the Western Australian Department of Water and Environmental Regulation (DWER) and part of the Transform Peel program. This research also received funding from the European Union's Horizon 2020 research and innovation programme under the Marie Skłodowska-Curie grant agreement No 835852. The authors thank Todd Rasmussen and two unnamed reviewers for their reviews of the submitted version of the manuscript. The authors thank Luk Peeters and Yousef Beiraghdar Aghbelagh for reviews of an early version of the manuscript. The authors thank Carey Johnston (DWER) for assistance in obtaining non-barometric pressure-corrected groundwater pressure data. The authors thank Margaret Shanafield for her assistance in testing of the regression deconvolution method.

Authors' Note

The author(s) does not have any conflicts of interest.

References

- Acworth, R.I., G.C. Rau, L.J. Halloran, and W.A. Timms. 2017. Vertical groundwater storage properties and changes in confinement determined using hydraulic head response to atmospheric tides. *Water Resources Research* 53, no. 4: 2983–2997.
- Acworth, R.I., L.J. Halloran, G.C. Rau, M.O. Cuthbert, and T.L. Bernardi. 2016. An objective frequency domain method for quantifying confined aquifer compressible storage using Earth and atmospheric tides. *Geophysical Research Letters* 43, no. 22: 11,671–11,678.
- Acworth, R.I., G.C. Rau, A.M. McCallum, M.S. Andersen, and M.O. Cuthbert. 2015. Understanding connected surface-water/groundwater systems using Fourier analysis of daily and sub-daily head fluctuations. *Hydrogeology Journal* 23, no. 1: 143–159.
- Acworth, R.I., and T. Brain. 2008. Calculation of barometric efficiency in shallow piezometers using water levels, atmospheric and earth tide data. *Hydrogeology Journal* 16, no. 8: 1469–1481.
- Arfken, G., and H. Weber. 2005. *Mathematical Methods for Physicists*, 6th ed., 1182. Boston, Massachusetts: Elsevier.
- Augustine, N.V.M. 2015. Estimating Specific Storage and Matrix Compressibility from Barometric Efficiency in

- the Southern Alberta Paskapoo Aquifer System. Master's thesis, University of Calgary, Calgary, Alberta, Canada, 408p.
- Barr, A.G., G. van der Kamp, R. Schmidt, and T.A. Black. 2000. Monitoring the moisture balance of a boreal aspen forest using a deep groundwater piezometer. *Agricultural and Forest Meteorology* 102, no. 1: 13–24.
- Beavan, J., K. Evans, S. Mousa, and D. Simpson. 1991. Estimating aquifer parameters from analysis of forced fluctuations in well level: An example from the Nubian formation near Aswan, Egypt: 2. Poroelastic properties. *Journal of Geophysical Research: Solid Earth* 96, no. B7: 12139–12160.
- Bernard, S., and F. Delay. 2008. Determination of porosity and storage capacity of a calcareous aquifer (France) by correlation and spectral analyses of time series. *Hydrogeology Journal* 16: 1299–1309.
- Bredehoeft, J.D. 1967. Response of well-aquifer systems to earth tides. *Journal of Geophysical Research* 72: 3075–3087.
- Burbey, T.J. 2010. Fracture characterization using Earth tide analysis. *Journal of Hydrology* 380, no. 3–4: 237–246.
- Burbey, T.J., D. Hisz, L.C. Murdoch, and M. Zhang. 2012. Quantifying fractured crystalline-rock properties using well tests, Earth tides and barometric effects. *Journal of Hydrology* 414: 317–328.
- Butler, J.J., W. Jin, G.A. Mohammed, and E.C. Reboulet. 2011. New insights from well responses to fluctuations in barometric pressure. *Groundwater* 49, no. 4: 525–533.
- Clark, W.E. 1967. Computing the barometric efficiency of a well. *Journal of the Hydraulics Division* 93, no. 4: 93–98.
- Cooper, H.H., J.D. Bredehoeft, I.S. Papadopoulos, and R.R. Bennett. 1965. The response of well-aquifer systems to seismic waves. *Journal of Geophysical Research* 70, no. 16: 3915–3926.
- Cooper, H.H., and C.E. Jacob. 1946. A generalized graphical method for evaluating formation constants and summarizing well-field history. *Eos Transactions of the American Geophysical Union* 27, no. 4: 526–534.
- Cuttillo, P.A., and J.D. Bredehoeft. 2011. Estimating aquifer properties from the water level response to Earth tides. *Groundwater* 49, no. 4: 600–610.
- Darner, R.A., and R.A. Sheets. 2012. Using existing data to estimate aquifer properties, Great Lakes region, USA. *Groundwater* 50, no. 3: 477–484.
- David, K., W.A. Timms, S.L. Barbour, and R. Mitra. 2017. Tracking changes in the specific storage of overburden rock during longwall coal mining. *Journal of Hydrology* 553: 304–320.
- Davidson, W.A., and X. Yu. 2008. Perth regional aquifer modelling system (PRAMS) model development: Hydrogeology and groundwater modelling, Western Australia Department of Water, Hydrogeological Record Series, Report No. HG 20.
- Davis, D.R., and T.C. Rasmussen. 1993. A comparison of linear regression with Clark's method for estimating barometric efficiency of confined aquifers. *Water Resources Research* 29, no. 6: 1849–1854.
- Desbarats, A.J., D.R. Boyle, M. Stapinsky, and M.J.L. Robin. 1999. A dual-porosity model for water level response to atmospheric loading in wells tapping fractured rock aquifers. *Water Resources Research* 35, no. 5: 1495–1505.
- Detournay, E., and A.H.-D. Cheng. 1993. Fundamentals of poroelasticity. In *Comprehensive Rock Engineering: Principles, Practice and Projects, Vol. II, Analysis and Design Method*, ed. C. Fairhurst, 113–171. Oxford, UK: Pergamon Press.
- Doodson, A.T., and H.C. Warburg. 1941. *Admiralty Manual of Tides*. London, UK: His Majesty's Stationery Office.
- Domenico, P.A., and F.W. Schwartz. 1990. *Physical and Chemical Hydrogeology*. New York: John Wiley and Sons.
- Domenico, P.A., and M.D. Mifflin. 1965. Water from low-permeability sediments and land subsidence. *Water Resources Research* 1, no. 4: 563–576.
- Dong, L., J. Shimada, M. Kagabu, and H. Yang. 2015. Barometric and tidal-induced aquifer water level fluctuation near the Ariake Sea. *Environmental Monitoring and Assessment* 187, no. 1: 4187.
- Ferris, J.G. 1952. Cyclic fluctuations of water level as a basis for determining aquifer transmissibility. *International Association of Scientific Hydrology* 33: 148–155. <https://doi.org/10.3133/70133368>
- Fileccia, A. 2011. Correcting water level data for barometric pressure fluctuations: Theoretical approach and a case history for an unconfined karst aquifer (Otavi, Namibia). *Acque Sotterranee (Italian Journal of Groundwater)* 126: 23–44.
- Fischer, G.J. 1992. Chapter 8: The determination of permeability and storage capacity: Pore pressure oscillation method. In *Fault Mechanics and Transport Properties of Rocks: A Festschrift in Honor*. International Geophysics Series 51, ed. W.F. Brace, B. Evans, and T.-F. Wong, 187–211. London, UK: Academic Press.
- Fuentes-Arreazola, M.A., J. Ramírez-Hernández, and R. Vázquez-González. 2018. Hydrogeological properties estimation from groundwater level natural fluctuations analysis as a low-cost tool for the Mexicali Valley aquifer. *Water* 10, no. 5: 586.
- Furbish, D.J. 1991. The response of water level in a well to a time series of atmospheric loading under confined conditions. *Water Resources Research* 27, no. 4: 557–568.
- Galloway, D., and S. Rojstaczer. 1988. Analysis of the frequency response of water-level altitudes in wells to Earth tides and atmospheric loading. In *Proceedings Fourth Canadian/American Conference on Hydrogeology, Fluid Flow, Heat Transfer, and Mass Transport in Fractured Rocks*, June 21–24, Banff, Alberta, ed. B. Hitchon and S. Bachu, 100–113. Dublin, Ohio: National Water Well Association.
- Geldon, A.L., Earle, J.D., and A.M.A. Umari. 1997. Determination of barometric efficiency and effective porosity, Boreholes UE-25 c#1, UE-25 c#2, and UE-25 c#3, Yucca Mountain, Nye County, Nevada. Water Resources Investigations Report 97–4098, United States Geological Survey, Denver, Colorado, 21p.
- Gonthier, G. J. 2007. A graphical method for estimation of barometric efficiency from continuous data—Concepts and application to a site in the piedmont, Air Force Plant 6, Marietta, Georgia. Scientific Investigations Report 2007–5111. Reston, Virginia: United States Geological Survey.
- Green, D.H., and H.F. Wang. 1990. Specific storage as a poroelastic coefficient. *Water Resources Research* 26, no. 7: 1631–1637.
- Hare, P.W., and R.E. Morse. 1999. Monitoring the hydraulic performance of a containment system with significant barometric pressure effects. *Groundwater* 37, no. 5: 755–763.
- Hare, P.W., and R.E. Morse. 1997. Water-level fluctuations due to barometric pressure changes in an isolated portion of an unconfined aquifer. *Groundwater* 35, no. 4: 667–671.
- He, A., R.P. Singh, Z. Sun, Q. Ye, and G. Zhao. 2016. Comparison of regression methods to compute atmospheric pressure and earth tidal coefficients in water level associated with Wenchuan earthquake of 12 May 2008. *Pure and Applied Geophysics* 173, no. 7: 2277–2294.
- Hobbs, P.J., and J.H. Fourie. 2000. Earth tide and barometric influences on the potentiometric head in a dolomite aquifer near the Vaal River Barrage, South Africa. *Water SA* 26, no. 3: 353–360.
- Hussein, M.E., N.E. Odling, and R.A. Clark. 2013. Borehole water level response to barometric pressure as an indicator

- of aquifer vulnerability. *Water Resources Research* 49, no. 10: 7102–7119.
- Hvorslev, M.J. 1951. Time lag and soil permeability in groundwater observations. Bulletin 36, United States Army Engineers Waterways Experiment Station, Vicksburg, Mississippi, 50p.
- Jacob, C.E. 1940. On the flow of water in an elastic artesian aquifer. *Transactions of the American Geophysical Union part 2*: 574–586.
- McMillan, T.C., G.C. Rau, W.A. Timms, and M.S. Andersen. 2019. Utilizing the impact of Earth and atmospheric tides on groundwater systems: A review reveals the future potential. *Reviews of Geophysics* 57, no. 2: 281–315.
- van der Kamp, G., and R. Schmidt. 2017. Review: Moisture loading—The hidden information in groundwater observation well records. *Hydrogeology Journal* 25: 2225–2233.
- van der Kamp, G., and J.E. Gale. 1983. Theory of Earth tide and barometric effects in porous formations with compressible grains. *Water Resources Research* 19, no. 2: 538–544.
- Kanasewich, E.R. 1981. *Time sequence analysis in geophysics*, 3rd ed., 480. Edmonton, Alberta: University of Alberta Press.
- Kilroy, K.C. 1992. Aquifer storage characteristics of Paleozoic carbonate rocks in southeastern Nevada estimated from harmonic analysis of water-level fluctuations. Doctoral dissertation, University of Nevada, Reno, Nevada, 84p.
- Larroque, F., O. Cabaret, O. Atteia, A. Dupuy, and M. Franceschi. 2013. Vertical heterogeneities of hydraulic aquitard parameters: Preliminary results from laboratory and in situ monitoring. *Hydrological Sciences Journal* 58, no. 4: 912–929.
- Larocque, M., A. Mangin, M. Razack, and O. Banton. 1988. Contribution of correlation and spectral analyses to the regional study of a large karst aquifer (Charente, France). *Journal of Hydrology* 205: 217–231.
- Lee, J.Y., and K.K. Lee. 2000. Use of hydrologic time series data for identification of recharge mechanism in a fractured bedrock aquifer system. *Journal of Hydrology* 229, no. 3–4: 190–201.
- Levenberg, K. 1944. A method for the solution of certain non-linear problems in least squares. *Quarterly of Applied Mathematics* 2, no. 2: 164–168.
- Marquardt, D.W. 1963. An algorithm for least-squares estimation of nonlinear parameters. *Journal of the Society for Industrial and Applied Mathematics* 11, no. 2: 431–441.
- McMillan, T.C., G.C. Rau, W.A. Timms, and M.S. Andersen. 2019. Utilizing the impact of Earth and atmospheric tides on groundwater systems: A review reveals the future potential. *Reviews of Geophysics* (in press). <https://doi.org/10.1029/2018RG000630>
- Melchior, P.J. 1983. *The Tides of the Planet Earth*. Oxford, Oxfordshire, UK: Pergamon Press, 641p.
- Merritt, M. L. 2004. Estimating hydraulic properties of the Floridan aquifer system by analysis of Earth-tide, ocean-tide, and barometric effects, Collier and Hendry Counties, Florida. Water Resources Investigations Report 03-4267. Tallahassee, Florida: United States Geological Survey.
- Munk, W.H., and G.J.F. MacDonald. 1960. *The Rotation of the Earth: A Geophysical Discussion*, 323. London, UK: Cambridge University Press.
- Odling, N.E., R.P. Serrano, M.E.A. Hussein, M. Riva, and A. Guadagnini. 2015. Detecting the vulnerability of groundwater in semi-confined aquifers using barometric response functions. *Journal of Hydrology* 520: 143–156.
- Padilla, A., and A. Pulido-Bosch. 1995. Study of hydrographs of karstic aquifers by means of correlation and cross-spectral analysis. *Journal of Hydrology* 168: 73–89.
- Palciauskas, V.V., and P.A. Domenico. 1989. Fluid pressures in deforming porous rocks. *Water Resources Research* 25, no. 2: 203–213.
- Peeters, L.J.M. 2017. Assumption hunting in groundwater modeling: Find assumptions before they find you. *Groundwater* 55, no. 5: 665–669.
- Quilty, E.G., and E.A. Roeloffs. 1991. Removal of barometric pressure response from water level data. *Journal of Geophysical Research: Solid Earth* 96, no. B6: 10209–10218.
- Rabiner, L.R., and B. Gold. 1975. *Theory and Application of Digital Signal Processing*, 762. Englewood Cliffs, New Jersey: Prentice-Hall.
- Rahi, K.A. 2010. Estimating the hydraulic parameters of the Arbuckle-Simpson aquifer by analysis of naturally-induced stresses. Doctoral dissertation, Oklahoma State University, Stillwater, Oklahoma.
- Rahi, K.A., and T. Halihan. 2013. Identifying aquifer type in fractured rock aquifers using harmonic analysis. *Groundwater* 51, no. 1: 76–82.
- Rahi, K. A. and T. Halihan. 2009. Estimating selected hydraulic parameters of the Arbuckle-Simpson aquifer from the analysis of naturally-induced stresses. Report for the Arbuckle-Simpson Hydrology Study. Stillwater, Oklahoma: Oklahoma State University.
- Rasmussen, T.C. 2005a. Tidal Efficiency. In *Water Encyclopedia*, ed. J.H. Lehr and J. Keeley. Hoboken, New Jersey: John Wiley and Sons. <https://doi.org/10.1002/047147844X.gw1166>
- Rasmussen, T.C. 2005b. Barometric efficiency. In *Water Encyclopedia*, ed. J.H. Lehr and J. Keeley. <https://doi.org/10.1002/047147844X.me21>
- Rasmussen, T.C., and T.L. Mote. 2007. Monitoring surface and subsurface water storage using confined aquifer water levels at the Savannah River Site, USA. *Vadose Zone Journal* 6, no. 2: 327–335.
- Rasmussen, T.C., and L.A. Crawford. 1997. Identifying and removing barometric pressure effects in confined and unconfined aquifers. *Groundwater* 35, no. 3: 502–511.
- Rau, G.C. 2018. *PyGTide: A Python Module and Wrapper for ETERNA PREDICT to Compute Synthetic Model Tides on Earth*. Karlsruhe, Germany: Institute of Applied Geosciences, Karlsruhe Institute of Technology. <https://doi.org/10.5281/zenodo.1346260>
- Rau, G.C., R.I. Acworth, L.J.S. Halloran, W.A. Timms, and M.O. Cuthbert. 2018. Quantifying compressible groundwater storage by combining cross-hole seismic surveys and head response to atmospheric tides. *Journal of Geophysical Research: Earth Surface* 123, no. 8: 1910–1930.
- Renard, P., D. Glenz, and M. Mejias. 2009. Understanding diagnostic plots for well-test interpretation. *Hydrogeology Journal* 17, no. 3: 589–600.
- Rhoads, G.H. Jr., and E.S. Robinson. 1979. Determination of aquifer parameters from well tides. *Journal of Geophysical Research* 84, no. B11: 6071–6082.
- Rice, J.R., and M.P. Cleary. 1976. Some basic stress diffusion solutions for fluid-saturated elastic porous media with compressible constituents. *Reviews of Geophysics and Space Physics* 14, no. 2: 227–241.
- Robinson, E.S., and R.T. Bell. 1971. Tides in confined well-aquifer systems. *Journal of Geophysical Research* 76, no. 8: 1857–1869.
- Robson, S.G., and E.R. Banta. 1990. Determination of specific storage by measurement of aquifer compression near a pumping well. *Groundwater* 28, no. 6: 868–874.
- Rojstaczer, S. 1988. Determination of fluid flow properties from the response of water levels in wells to atmospheric loading. *Water Resources Research* 24, no. 11: 1927–1938.
- Sahu, P. 2004. Use of time series, barometric and tidal analyses to conceptualise and model flow in an underground mine: The Corning Mine Complex, Ohio. Master's thesis, Ohio University, Athens, Ohio.
- Saltelli, A., A.G. Pereira, J.P. van der Sluijs, and S. Funtowicz. 2013. What do I make of your latinorum? Sensitivity

- auditing of mathematical modelling. *International Journal of Foresight and Innovation Policy* 9: 213–234.
- Seo, H.H. 1999. Modeling the response of groundwater levels in wells to changes in barometric pressure. Doctoral dissertation, Iowa State University, Ames, Iowa.
- Skempton, A.W. 1954. The pore-pressure coefficients A and B. *Geotechnique* 4, no. 4: 143–147.
- Smerdon, B.D., L.A. Smith, G.A. Harrington, W.P. Gardner, C. Delle Piane, and J. Sarout. 2014. Estimating the hydraulic properties of an aquitard from in situ pore pressure measurements. *Hydrogeology Journal* 22, no. 8: 1875–1887.
- Smith, L.A., G. van der Kamp, and M.J. Hendry. 2013. A new technique for obtaining high-resolution pore pressure records in thick claystone aquitards and its use to determine in situ compressibility. *Water Resources Research* 49, no. 2: 732–743.
- Spane, F.A., and R.D. Mackley. 2011. Removal of river-stage fluctuations from well response using multiple regression. *Groundwater* 49, no. 6: 794–807.
- Theis, C.V. 1935. The relation between the lowering of the piezometric surface and the rate and duration of discharge of a well using ground-water storage. *Eos Transactions of the American Geophysical Union* 16, no. 2: 519–524.
- Timms, W.A., and R.I. Acworth. 2005. Propagation of pressure change through thick clay sequences: An example from Liverpool Plains, NSW, Australia. *Hydrogeology Journal* 13, no. 5–6: 858–870.
- Veatch, A.C. 1906. Fluctuations of the water level in wells, with special reference to Long Island, New York. Water Supply and Irrigation Paper No. 155. Washington, DC: United States Geological Survey, Government Printing Office.
- Wang, H.F. 2000. *Theory of Linear Poroelasticity With Applications to Geomechanics and Hydrogeology*. Princeton, New Jersey: Princeton University Press.
- Weeks, E.P. 1979. Barometric fluctuations in wells tapping deep unconfined aquifers. *Water Resources Research* 15, no. 5: 1167–1176.
- Welch, P. 1967. The use of fast Fourier transform for the estimation of power spectra: A method based on time averaging over short, modified periodograms. *IEEE Transactions on Audio and Electroacoustics* 15, no. 2: 70–73.
- Yew, C.H., and P.N. Jogi. 1977. The determination of Biot's parameters for sandstones part 1: Static tests. *Experimental Mechanics* 18, no. 5: 167–172.

Repository KITopen

Dies ist ein Postprint/begutachtetes Manuskript.

Empfohlene Zitierung:

Turnadge, C.; Crosbie, R. S.; Barron, O.; Rau, G. C.

[Comparing methods of barometric efficiency characterisation for specific storage estimation](#).

2019. Groundwater, 57.

[doi: 10.554/IR/1000096934](https://doi.org/10.554/IR/1000096934)

Zitierung der Originalveröffentlichung:

Turnadge, C.; Crosbie, R. S.; Barron, O.; Rau, G. C.

[Comparing methods of barometric efficiency characterisation for specific storage estimation](#).

2019. Groundwater, 57 (6), 844–859.

[doi:10.1111/gwat.12923](https://doi.org/10.1111/gwat.12923)

Lizenzinformationen: [KITopen-Lizenz](#)